Photoreductive Mechanism of CCl4 Degradation on TiO2 Particles and Effects of Electron Donors

ARTICLE *in* ENVIRONMENTAL SCIENCE AND TECHNOLOGY · JUNE 1995

Impact Factor: 5.33 · DOI: 10.1021/es00006a031 · Source: PubMed

2 AUTHORS:

Wonyong Choi
Pohang University of Science and Technology
256 PUBLICATIONS **23,664** CITATIONS
SEE PROFILE

Michael R. Hoffmann
California Institute of Technology
378 PUBLICATIONS **30,068** CITATIONS
SEE PROFILE

Kinetics and Mechanism of CCl_4 Photoreductive Degradation on TiO_2: The Role of Trichloromethyl Radical and Dichlorocarbene

Wonyong Choi and Michael R. Hoffmann*

W. M. Keck Laboratories, California Institute of Technology, Pasadena, California 91125

Received: May 23, 1995; In Final Form: October 30, 1995[⊗]

The mechanism of photoreduction of CCl_4 on illuminated TiO_2 surfaces was investigated by selectively trapping transient free radical intermediates. Dichlorocarbene and trichloromethyl radical were trapped with 2,3-dimethyl-2-butene during the photocatalytic degradation of CCl_4. The rate of formation of trapped $:CCl_2$ and $^{\bullet}CCl_3$ was found to be a function of $[H_2O]$, pH, $[CCl_4]$, the nature of the dissolved gas, and light intensity. Dissolved oxygen was not essential for the degradation of CCl_4. The production rate of trapped dichlorocarbene showed light intensity dependencies of second, first, and half order with progressively increasing light intensity. A two-electron photoreductive pathway (via dichlorocarbene formation) was found to be the dominant mechanism leading to the full degradation of CCl_4. Since dichlorocarbene is hydrolyzed under basic conditions, the pH and water concentration were found to be integral parameters controlling the complete degradation of CCl_4 to CO, CO_2, and HCl. Kinetic equations describing the formation of trapped dichlorocarbene were derived from a proposed mechanism. The comparison of the predicted rate expression to the observed data suggested that the observed two-electron transfer occurred consecutively.

Introduction

Semiconductor photocatalysis has been intensively studied and investigated for a wide variety of applications such as water splitting,[1] organic chemical synthesis,[2] metal recovery,[3] and water and air treatment.[4] Among the wide-band-gap semiconductors, TiO_2 is the most widely used due to its outstanding photostability.[5] In particular, its application to hazardous waste remediation has emerged as a viable technology.

In colloidal TiO_2, both the photogenerated electrons and holes are likely transferred to substrates at the solid/liquid interface.[6] While hole-transfer reactions (i.e., photooxidation) have been widely studied due to the strong oxidation potential ($E^{\circ} = +2.7$ V vs NHE at pH 7) of the valence-band edge of TiO_2, electron-transfer reactions have been investigated primarily as an auxiliary step to minimize charge-pair recombination. Not many studies on chemistry induced by photoelectron transfer on TiO_2 are found.[6−10]

Carbon tetrachloride degradation is initiated by a one-electron reduction step that may be followed by a series of oxidation or reduction steps. The degradation of CCl_4 has been studied using γ-ray radiolysis,[11] TiO_2 photocatalysis,[7b] sonolysis,[12] electrolysis,[13,14] and photolysis on MgO.[15] In addition, CCl_4 reduction is known to occur in aquatic environments in the presence of mineral surfaces[16] and on iron powders.[17] In a recent study,[18] we demonstrated that CCl_4 can be photochemically degraded through the mechanism involving photoreduction by conduction-band electrons in the presence of TiO_2 and suitable electron donors. On the basis of the fact that CCl_4 was found to be fully degraded in the absence of dissolved oxygen,[18] we also suggested that the initial electron-transfer process may involve both one- and two-electron transfer reactions. The one- and two-electron steps result in the formation of trichloromethyl radical and dichlorocarbene as intermediates, respectively. Both pathways result in the release of chloride ions (dissociative electron capture).

$$CCl_4 + e_{cb}^{-} \rightarrow {}^{\bullet}CCl_3 + Cl^{-} \quad (1)$$

$$CCl_4 + 2e_{cb}^{-} \rightarrow :CCl_2 + 2Cl^{-} \quad (2)$$

In this study, we present direct evidence for competing one- and two-electron-transfer steps to CCl_4 by trapping the short-lived intermediates. The transient intermediates were trapped using 2,3-dimethyl-2-butene as follows:

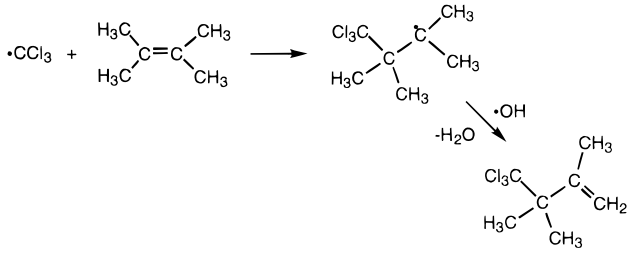

(3)

(4)

The product of reaction 3, $C_7H_{11}Cl_3$ (4,4,4-trichloro-2,3,3-trimethyl-1-butene) will be referred to as TCCl3, and that of reaction 4, $C_7H_{12}Cl_2$ (1,1-dichloro-2,2,3,3-tetramethylcyclopropane), as TCCl2. In this paper, we examine the kinetics of the formation of TCCl3 and TCCl2 and propose a mechanism for CCl_4 photodegradation consistent with our kinetic observations.

Experimental Section

Titanium dioxide (Degussa P25), which is a known mixture of 80% anatase and 20% rutile with an average particle size of 30 nm and a reactive surface area of ~50 m^2/g, was used as a photocatalyst without further treatment. TiO_2 concentrations were maintained at 0.5 g/L in all experiments. To explore the

* To whom correspondence should be addressed.

[⊗] Abstract published in *Advance ACS Abstracts,* January 1, 1996.

0022-3654/96/20100-2161$12.00/0

effects of dissolved gas (Figure 4), the particle suspensions were bubbled with O_2, air, and N_2, respectively, for 30−40 min before addition of the trapping agent and CCl_4. The pH of the suspension was adjusted with 1 N $HClO_4$ or 1 N NaOH. CCl_4 (Baker) and 2,3-dimethyl-2-butene (Aldrich) were used as received.

Steady-state photolyses were performed with a 1000-W Xe arc lamp (Spindler and Hoyer). Light was filtered through a 10-cm IR water filter and a UV band-pass filter (310−400 nm, Corning). The filtered light was focused onto a 35-mL quartz reactor cell loaded with TiO_2 suspension. The head space above the suspension was minimized. Light intensity measurements were performed by chemical actinometry using (*E*)-α-((2,5-dimethyl-3-furyl)ethylidene)isopropylidenesuccinic anhydride (Aberchrome 540).[19] The typical light intensity was $\sim 1.4 \times 10^{-3}$ einstein L^{-1} min^{-1}. Two types of photolysis experiments were carried out. Detection of TCCl3 and TCCl2 was carried out in a water/acetonitrile mixture in order to increase the solubility of 2,3-dimethyl-2-butene (trap) and CCl_4 up to 100 and 10 mM, respectively. Water concentrations were varied from 0 to 10 M. In order to investigate the degradation of CCl_4, photolyses were carried out in aqueous suspensions in the presence of methanol and 2-propanol (0.1 M) as electron donors. The desired concentrations of CCl_4 in water were prepared by dilution of a saturated CCl_4 stock solution (5.1 mM).

Sample aliquots were obtained with a 1-mL syringe, filtered through a 0.45-μm nylon filter, and injected into a 2.5-mL glass vial with a PTFE/silicone septum-lined threaded cap. CCl_4 and intermediates were extracted with 0.5 mL of pentane immediately after sampling. Sample vials were stored at 4 °C in the dark up to 48 h before analysis. CCl_4 degradation, the formation of intermediates, and the formation of products were followed chromatographically with a Hewlett−Packard (HP) 5880A gas chromatograph (GC) equipped with a ^{63}Ni electron capture detector and a HP-5 column (cross-linked 50% PhMe silicone, 25 m × 0.32 mm × 1.05 μm). Nitrogen was used as the carrier gas. For the detection and identification of TCCl3 and TCCl2, a HP 5890 II gas chromatograph with a HP-5 column serially connected to a HP 5965B infrared detector (IRD) and a HP 5972A mass selective detector (MSD) was used. The carrier gas, in this case, was helium. The GCs were calibrated daily with external standards, and duplicate measurements were made for each sample. The bottom aqueous phase (or water/acetonitrile phase) in the sampling vial was analyzed by ion-exchange chromatography (IC) for Cl^- ion. The IC system was a Dionex Bio-LC system equipped with a conductivity detector and a Dionex OmniPac PAX-500 column (8 μm × 5 mm × 250 mm).

1,1-Dichloro-2,2,3,3-tetramethylcyclopropane (TCCl2) was synthesized using the method of Doering and Henderson.[20] The product was a white powder having a melting range of 51.0−51.5 °C. No significant impurity was detected by GC/MS. Since authentic samples of 4,4,4-trichloro-2,3,3-trimethyl-1-butene (TCCl3) were not available, its quantification was prevented. However, analyses of mass and FTIR spectra provided sufficient information to identify the formation of TCCl3. The formation of TCCl2 and TCCl3 was followed by monitoring mass signals of $m/e = 131$ and $m/e = 165$, respectively. These peaks represented fragment ions of the molecular ion less chlorine atom ($m/e = M - 35$).

Results

Formation of TCCl2 and TCCl3 and Degradation of CCl_4. The mass spectra of TCCl2 and TCCl3, which were generated during the photolysis of CCl_4 in the presence of 2,3-dimethyl-2-butene (trap), are shown in Figure 1. The molecular ion peak of TCCl2 ($m/e = 166$) was too weak to be detected at its in-situ concentration (<5 μM). However, the GC retention time and mass spectrum of TCCl2 exactly matched those of the authentic compound. In the case of TCCl3, the relative intensity ratios of the chlorine isotope peaks at masses M, $M + 2$, and $M + 4$ were 3:3:1, which indicated that three chlorine atoms were contained in the molecular ion.[21] The presence of the terminal C═C double bond was confirmed by the FTIR spectrum, which showed a C═C stretching vibration at 1630 cm^{-1} and an olefinic C−H stretching vibration at 3109 cm^{-1}.

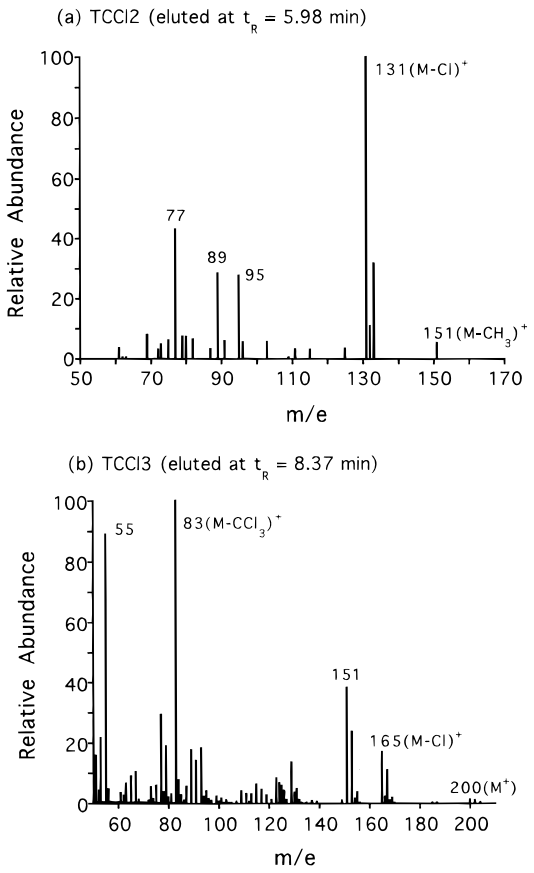

Figure 1. Mass spectra (extracted from a GC total ion chromatogram) of (a, top) TCCl2 and (b, bottom) TCCl3 which were generated during the CCl_4 photolysis in the presence of TiO_2 and traps. The mass signal intensities were normalized.

The production of TCCl2 during photolysis was linear up to 30 min, as shown in Figure 2. TCCl3 production showed a similar trend. Most of data shown in this paper were reproducible within ±10%. The production of trapped intermediates appeared to depend on $[H_2O]$. This effect is shown in Figure 3. Production of both TCCl2 and TCCl3 increased with increasing water concentration up to 1 M. However, further increases in the water concentration resulted in a reduced production of TCCl2, while TCCl3 production continued to increase slowly. On the other hand, chloride production was found to be significant only in an excess of water (10 M). The production of Cl^- at lower water concentrations (≤1 M) in Figure 3 was negligible although the production of TCCl2 and TCCl3 was a clear indication of chloride production. The chloride production corresponding to the formation of TCCl2 at $[H_2O] = 1$ M was ~7 μM. As for TCCl3, a similar amount of chloride was expected to be generated even though the concentration of TCCl3 was not determined. Therefore, the total chloride production at $[H_2O] = 1$ M may not exceed 20 μM, which is similar to the *in-situ* chloride impurity concentration

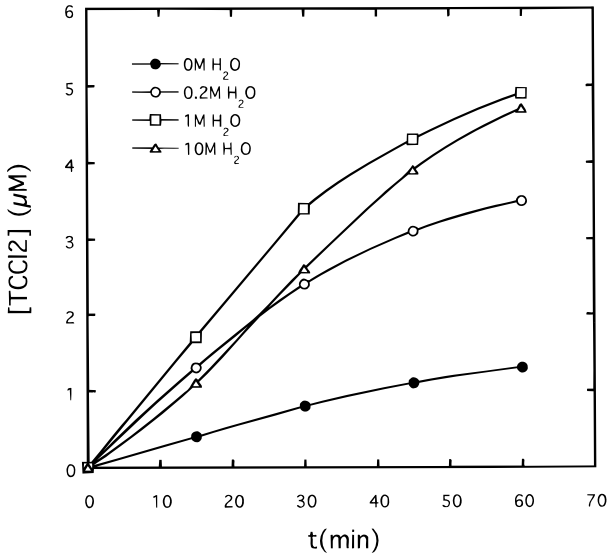

Figure 2. Time-dependent production of TCCl2 during the photolysis with varying amounts of water (0, 0.2, 1, and 10 M). The experimental conditions were: $[CCl_4]_0 = 5$ mM, $[TiO_2] = 0.5$ g L^{-1}, $I = 1.43 \times 10^{-3}$ einstein L^{-1} min^{-1} ($310 < \lambda < 400$ nm), [trap] = 0.1 M, air equilibration, and no pH adjustment.

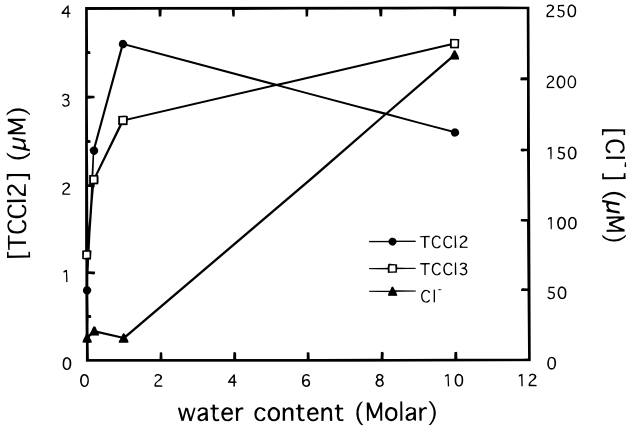

Figure 3. Comparison of the production of TCCl2, TCCl3, and chloride after a 30 min irradiation as a function of water concentration in TiO_2 suspension. Other experimental conditions were the same as those of Figure 2. The concentration of TCCl3 was not determined.

in the TiO_2 (Degussa P25) suspension. At such low [Cl^-], the titania surface can serve as a buffer site, retaining the additional chloride produced. Such a retention can be significant when the dielectric constant of the solution (mostly acetonitrile) is low.

Since dissolved O_2 is an alternative electron acceptor competing with CCl_4 and since it is known to react fast with $\bullet CCl_3$, the effect of dissolved oxygen on the formation of TCCl2 and TCCl3 was investigated. In Figure 4, the production of TCCl2 and TCCl3 in illuminated TiO_2 suspensions, which were sparged with nitrogen, air, and oxygen prior to photoirradiation, is compared. In the presence of O_2, the apparent induction period increased with increasing [O_2]. This trend is consistent with the effect of scavenging CB electrons by O_2. The appearance of an induction period in the N_2-saturated system can be attributed to surface adsorbed oxygen, which was not readily removed by purging alone. After the induction period, during which oxygen was consumed, the production rate of TCCl2 and TCCl3 in the O_2-saturated system increased to the level of the oxygen-free system. In the case of TCCl2 production, there was little difference between N_2- and air-saturated solutions except for the initial induction period. However, TCCl3

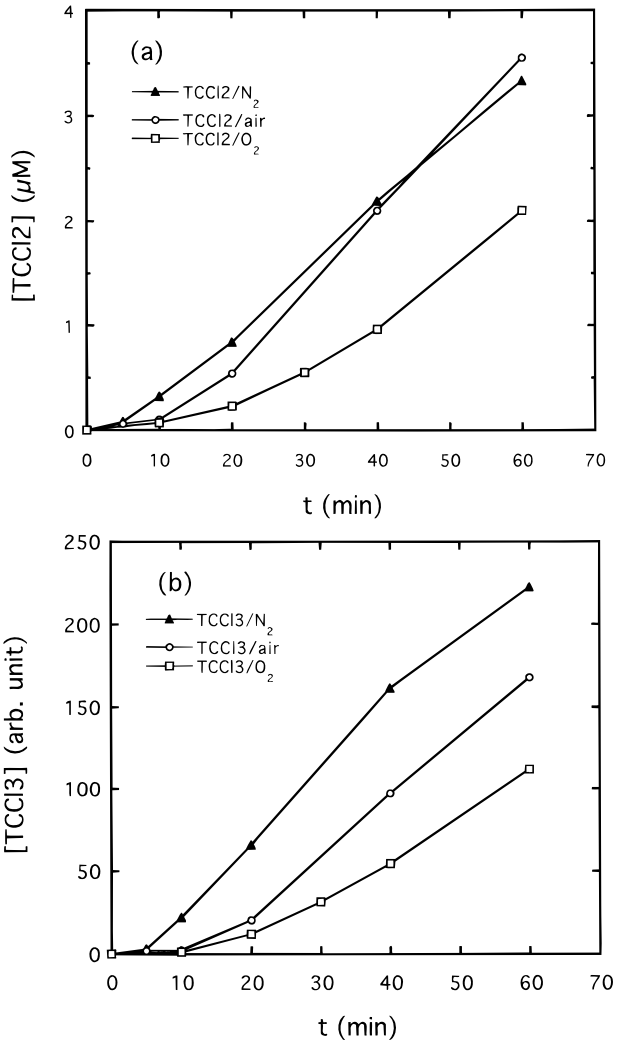

Figure 4. Production of (a, top) TCCl2 and (b, bottom) TCCl3 as a function of irradiation time in TiO_2 suspensions saturated with N_2, air, and O_2 gases before irradiation. Water concentration was 10 M, and other experimental contions were the same as those of Figure 2.

production in an air-saturated suspension was significantly delayed compared with its production in a N_2-saturated suspension.

The influence of $[CCl_4]_0$ on the production rates of TCCl2 and TCCl3 is compared for two different light intensities in Figure 5. The production of TCCl2 showed similar saturation behavior at both low (6.1×10^{-5} einstein L^{-1} min^{-1}) and high (1.4×10^{-3} einstein L^{-1} min^{-1}) light intensities. However, the production rate of TCCl3 at the lower light intensity reached a saturation level sooner than the system at high light intensity. The solid lines are fits to a Langmuir−Hinshelwood equation ($\nu = kK[CCl_4]/(1 + K[CCl_4])$). The corresponding constants for TCCl2 are k =155.7 nM min^{-1} and $K = 330$ M^{-1} for high light intensity and $k = 11.2$ nM min^{-1} and $K = 200$ M^{-1} for low light intensity.

The production rates of TCCl2 are plotted as a function of light intensity in Figure 6. Three distinct regions are apparent. Over a broad range, the light intensity dependence changes from $\nu_{TCCl2} \propto I^{2.0}$ ($I < 1.6 \times 10^{-4}$ einstein L^{-1} min^{-1}) to $\nu_{TCCl2} \propto I^{1.0}$ ($1.6 \times 10^{-4} < I < 3.5 \times 10^{-4}$ einstein L^{-1} min^{-1}) and finally to $\nu_{TCCl2} \propto I^{0.5}$ ($I > 3.5 \times 10^{-4}$ einstein L^{-1} min^{-1}). The measured rates in the third region appear to deviate from the square-root dependence. This may be due to light-scattering losses in the turbid suspension at higher light intensities. The average photon fluxes per particle at $I = 1.6 \times 10^{-4}$ and $3.5 \times$

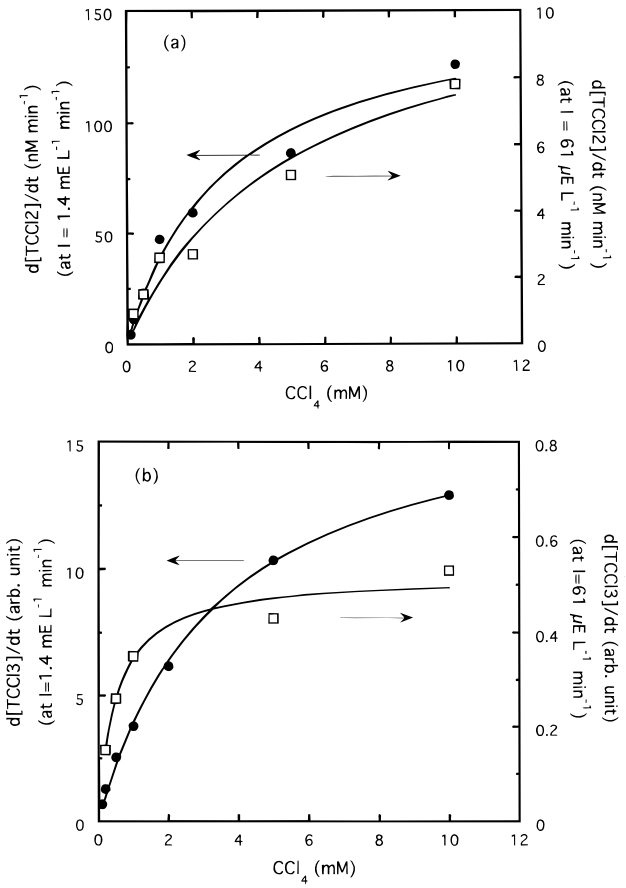

Figure 5. Production of (a, top) TCCl2 and (b, bottom) TCCl3 as a function of initial CCl_4 concentration. The concentration dependences are compared at two different light intensities (1400 vs 61 μE L^{-1} min^{-1}). Water concentration was 10 M, and other experimental contions were the same as those of Figure 2.

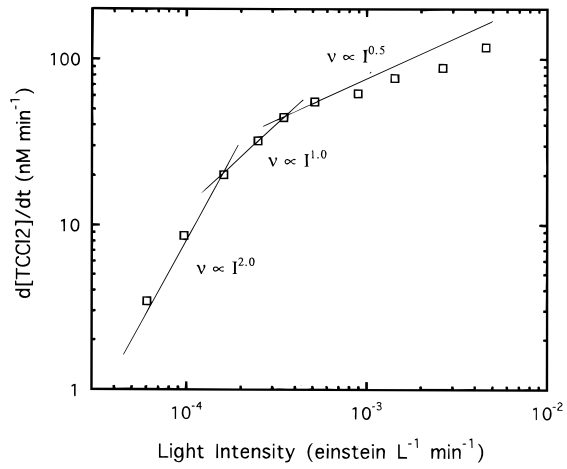

Figure 6. Light intensity dependence of TCCl2 production rate under the same experimental conditions of Figure 2. Water concentration was 10 M. The solid lines represent the light-intensity dependence of $I^{2.0}$, $I^{1.0}$, and $I^{0.5}$, respectively.

10^{-4} einstein L^{-1} min^{-1} (or 1.8×10^{-6} and 3.9×10^{-6} einstein cm^{-2} min^{-1}) are 176 and 385 photons/(particle•s), respectively (assuming an average particle size of 30 nm).

Such transition light intensities seem to vary with the experimental conditions. In our previous study[22] using the same photocatalyst (Degussa P25, 0.5 g/L), the photodegradation of chloroform showed the light intensity order transition at 6.87×10^{-5} einstein L^{-1} min^{-1}. As for Fe^{3+}-doped (0.5 atom %) quantum-sized TiO_2,[6b] the same photoreaction showed the

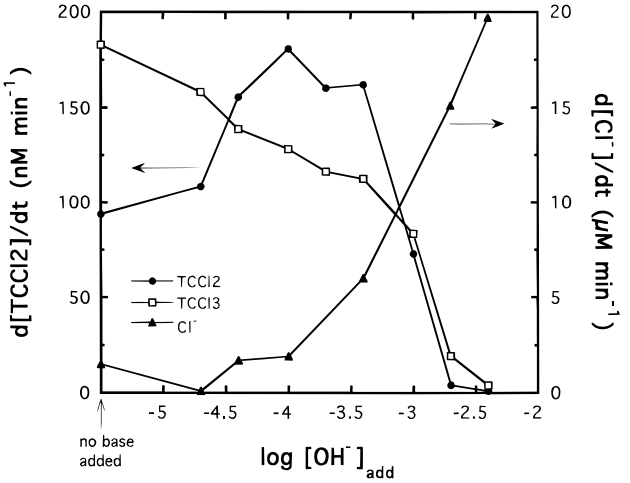

Figure 7. pH (relative scale) dependence of the production rate of TCCl2, TCCl3, and chloride in the TiO_2 suspension having the same conditions as those of Figure 2. Water concentration was 10 M. The production rate of TCCl3 is relative.

transition at 5.5×10^{-4} einstein L^{-1} min^{-1}. In a 2-propanol photooxidation study using pure rutile powder (10 g/L), Egerton and King[23a] reported the light intensity order changed from first order to half order at 1.2×10^{-5} einstein L^{-1} min^{-1}. On the other hand, Okamoto et al.[23b] showed that the light intensity dependence of phenol photooxidation using anatase (2 g/L) changed from first order to half order around $(1.7-3.4) \times 10^{-5}$ einstein L^{-1} min^{-1}.

The light intensity dependencies of TCCl3 production were also measured (data not shown due to the undetermined TCCl3 concentration) and showed the similar behavior of second-, first-, and half-order transition with increasing light intensity. Even though the production of TCCl3 requires only one electron (unlike TCCl2 which needs two electrons), it needs a hydroxyl radical (a hole-equivalent) instead (reaction 3). Therefore, the overall process of TCCl3 production is equivalent to the two-electron transfer in terms of the total number of charge transfer, which makes its light intensity dependence indistinguishable from that of TCCl2.

The formation of products and intermediates in TiO_2/UV-catalyzed reactions often shows a strong pH dependence. In order to investigate the effects of pH, the production rates of TCCl2, TCCl3, and Cl^- were measured as a function of pH (Figure 7). The absolute pH values of the suspensions were not given on the abscissa of Figure 7, since the reaction medium was a mixture of water and acetonitrile in which the proton activity was not measured.[24] However, the log $[OH^-]_{add}$ can be used as a surrogate for pH. The production rate of TCCl2 showed a maximum at log $[OH^-]_{add} \sim -4$ while that of TCCl3 monotonously decreased with increasing base concentration. Both production rates dropped quickly above log $[OH^-]_{add} > -3.5$. On the other hand, the chloride production rate, which provides a measure of total CCl_4 degradation, showed an anticorrelation with the production rate of TCCl2. The pH-dependent behavior was also investigated in an aqueous solution of CCl_4 (Figure 8), which were measured using a pH-stat titration technique.[18,25] This technique measured the consumption rate of the standard base (NaOH 0.10 N) titrant, which was added to the reactor in order to maintain the pH of the system constant. The acid generation resulting from CCl_4 degradation to HCl, which is equivalent to the base consumption during titration, can be considered as an indicator of CCl_4 degradation. The acid generation rate showed a drastic increase above pH 10. This behavior is also seen for Cl^- production, as shown in Figure 7.

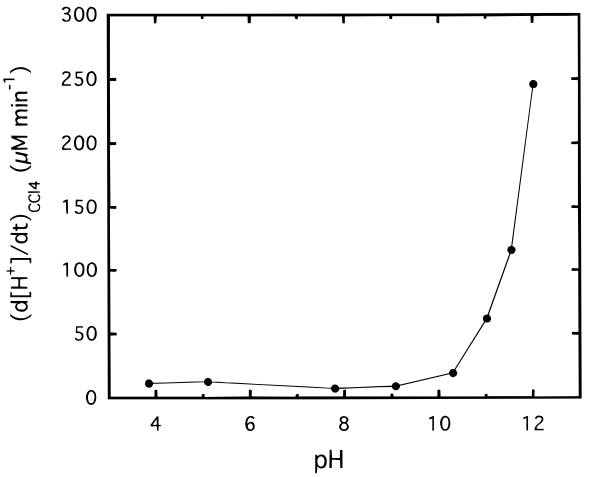

Figure 8. pH dependence of CCl_4 degradation, which was measured by monitoring the acid generation rate, in an aqueous TiO_2 suspension where $[CCl_4]_0 = 5.1$ mM, $[TiO_2] = 0.5$ g L^{-1}, $I = 2.1 \times 10^{-4}$ einstein L^{-1} min^{-1} ($\lambda = 320 \pm 10$ nm), $[CH_3OH] = 0.1$ M, and there is air-equilibration.

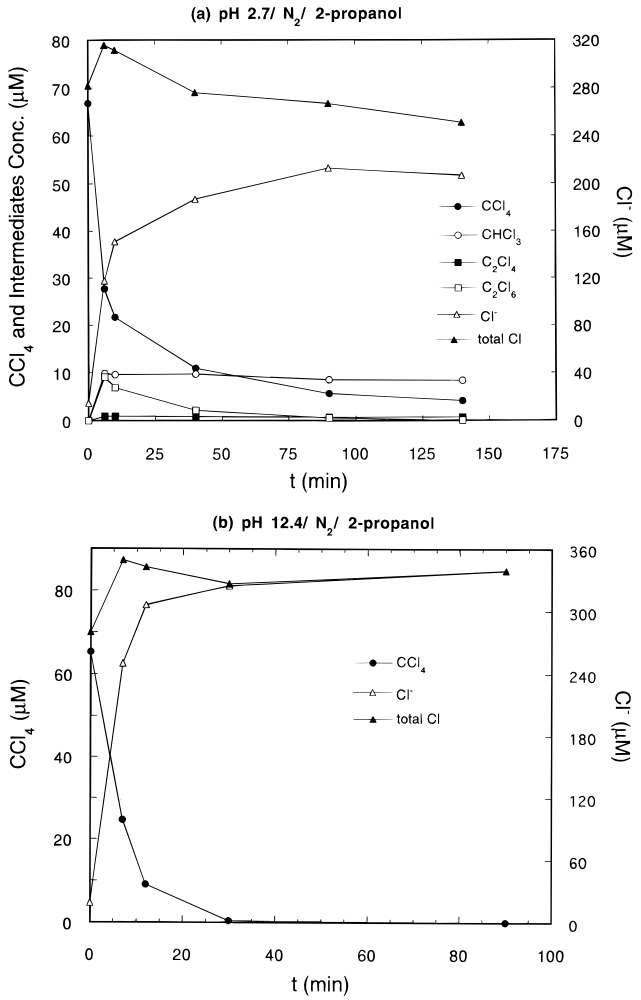

Figure 9. Degradation of CCl_4 and the production of intermediates and chloride in an aqueous TiO_2 suspension at (a, top) pH 2.7 and (b, bottom) pH 12.4. Other experimental conditions were $[TiO_2] = 0.5$ g L^{-1}, $I = 1.46 \times 10^{-3}$ einstein L^{-1} min^{-1} ($310 < \lambda < 400$ nm), $[(CH_3)_2CHOH] = 0.1$ M, and N_2 saturation prior to light illumination.

The product and intermediate analyses were also determined for photocatalytic CCl_4 degradation in aqueous TiO_2 suspensions at pH 2.7 (Figure 9a) and pH 12.4 (Figure 9b). At pH 2.7, intermediates such as $CHCl_3$, C_2Cl_4, and C_2Cl_6 were formed while no intermediates were detected at pH 12.4. The degradation of CCl_4 was found to be much faster at pH 12.4 than at pH 2.7.

TABLE 1: Elementary Reaction Steps of CCl_4 Photolysis in UV-Irradiated TiO_2

Photoexcitation	
$TiO_2 \xrightarrow{h\nu} e_{cb}^- + h_{vb}^+$	R1
Adsorption	
$CCl_4 + >S$ (surface site) $\leftrightarrow >CCl_{4,ad}$	R2
$O_2 + >S \leftrightarrow >O_{2,ad}$	R3
$T + >S \leftrightarrow T_{ad}$	R4
Electron Transfer	
$O_{2,ad} + e_{cb}^- \leftrightarrow O_2^-$	R5
$>Ti^{IV} + e_{cb}^- \leftrightarrow >Ti^{III}(\equiv e_{tr}^-)$	R6
$CCl_{4,ad} + e_{cb}^- \rightarrow {}^\bullet CCl_3 + Cl^-$	R7
$CCl_{4,ad} + >Ti^{III} \rightarrow {}^\bullet CCl_3 + Cl^-$	R8
${}^\bullet CCl_3 + e_{cb}^- \leftrightarrow CCl_3^-$	R9
${}^\bullet CCl_3 + >Ti^{III} \leftrightarrow CCl_3^-$	R10
$CCl_{4,ad} + 2e_{cb}^- \rightarrow CCl_3^- + Cl^-$	R11
$CCl_3^- \leftrightarrow :CCl_2 + Cl^-$	R12
Hole Transfer	
$h_{vb}^+ + H_2O$ (or $>TiOH$) $\rightarrow {}^\bullet OH$ (or $>TiOH^\bullet$) $+ H^+$	R13
${}^\bullet OH + DH \rightarrow D^\bullet + H_2O$	R14
Recombination	
$e_{cb}^- + h_{vb}^+ \rightarrow TiO_2$	R15
Intermediate and Product Formation	
$2{}^\bullet CCl_3 \rightarrow C_2Cl_6$	R16
${}^\bullet CCl_3 + DH \rightarrow CHCl_3 + D^\bullet$	R17
${}^\bullet CCl_3 + O_2 \rightarrow {}^\bullet OOCCl_3$	R18
${}^\bullet CCl_3 + T \rightarrow {}^\bullet TCCl3$	R19
${}^\bullet TCCl3 + {}^\bullet OH \rightarrow TCCl3 + H_2O$	R20
$CCl_3^- + H^+ \rightarrow CHCl_3$	R21
$2{:}CCl_2 \rightarrow C_2Cl_4$	R22
$:CCl_2 + T \rightarrow TCCl2$	R23
${}^\bullet OOCCl_3 \rightarrow\!\!\rightarrow CO_2 + 3Cl^-$	R24
$:CCl_2 + H_2O/OH^- \rightarrow CO + 2HCl$	R25
$CO + OH^- \rightarrow HCOO^-$	R26
$HCOO^- + {}^\bullet OH \rightarrow\!\!\rightarrow CO_2$	R27

Photochemical Mechanism of CCl_4 Degradation on TiO_2. We propose a detailed mechanism of CCl_4 photolysis in TiO_2 suspension that is listed in Table 1 in order to interpret our results. The intermediate trap (2,3-dimethyl-2-butene) is symbolized as T; DH indicates a suitable electron donor (i.e., trap, acetonitrile, alcohols) with abstractable hydrogen atoms. In this proposed mechanism, several assumptions are made: (i) adsorption equilibria for various intermediate species are omitted; (ii) only indirect hole transfers are considered; (iii) only recombination between free charge carriers is considered; (iv) the actual surficial reaction sites are not specified[26] (For example, the bimolecular reaction of reaction R23 can take place between two adsorbates (Hinshelwood-type) or between one adsorbate and the other in the solution (Rideal-type) or between both in the solution after desorption.); (v) the degradation reaction of TCCl2 is not shown because it is negligible in the presence of excess hole scavengers such as the trap during the initial portions of the reaction.

In addition to the above assumptions, we have to keep in mind that the following reactions are in competition with reactions 3 and 4:

$$ {}^\bullet CCl_3 + O_2 \rightarrow {}^\bullet OOCCl_3 \quad (5)$$

$$ 2{}^\bullet CCl_3 \rightarrow C_2Cl_6 \quad (6)$$

$$ {}^\bullet CCl_3 + CH_3CN \rightarrow CHCl_3 + {}^\bullet CH_2CN \quad (7)$$

$$:CCl_2 + H_2O \rightarrow CO + 2HCl \quad (8)$$

$$ 2{:}CCl_2 \rightarrow C_2Cl_4 \quad (9)$$

TABLE 2: Kinetic Rate Equations of TCCl2 Production for Three Different Cases of Electron Transfers to CCl_4

	$\frac{d[TCCl2]}{dt}$	
case	low light intensities	high light intensities
I $CCl_{4,ad} + e_{cb}^-$ $^{\bullet}CCl_3 + e_{cb}^-$	$k_{1L}I_{abs}^2[CCl_{4,ad}]$ where $k_{1L} = \frac{k_a k_{R23} k_{R7} f_1([H^+])^a}{k'^2_{R13}\sum k_i[S_i]}[T]$	$k_{1H}I_{abs}^{1/2}[CCl_{4,ad}]$ where $k_{1H} = \frac{k_a k_{R23} k_{R7} f_1([H^+])}{k_{R9} k_{R15}^{1/2}}[T]$
II $CCl_{4,ad} + 2e_{cb}^-$	$k_{2L}I_{abs}^2[CCl_{4,ad}]$ where $k_{2L} = \frac{k_a k_{R23} f_2([H^+])^b}{k'^2_{R13}}[T]$	$k_{2H}I_{abs}[CCl_{4,ad}]$ where $k_{2H} = \frac{k_a k_{R23} f_2([H^+])}{k_{R15}}[T]$
III $CCl_{4,ad} + >Ti^{III}$ $^{\bullet}CCl_3 + >Ti^{III}$	$k_{3L}I_{abs}^2 \frac{\frac{k_{R8}}{k_{-R6}}[CCl_{4,ad}]}{\left(1 + \frac{k_{R8}}{k_{-R6}}[CCl_{4,ad}]\right)^2}$ where $k_{3L} = \frac{k_a k_{R23} k_{R6}^2 f_3([H^+])^c}{k'^2_{R13} k_{-R6}\sum k_i[S_i]}[Ti^{IV}]^2[T]$	$k_{3H}I_{abs}^{1/2} \frac{\frac{k_{R8}}{k_{-R6}}[CCl_{4,ad}]}{\left(1 + \frac{k_{R8}}{k_{-R6}}[CCl_{4,ad}]\right)}$ where $k_{3H} = \frac{k_a k_{R23} k_{R6} f_3([H^+])}{k_{R10} k_{R15}^{1/2}}[Ti^{IV}][T]$

[a] $f_1([H^+]) = \frac{k_{R9}}{k_{-R9} + k_{R12} + k_{R21}[H^+]}$. [b] $f_2([H^+]) = \frac{k_{R11}}{k_{-R9} + k_{R12} + k_{R21}[H^+]}$. [c] $f_3([H^+]) = \frac{k_{R10}}{k_{-R10} + k_{R12} + k_{R21}[H^+]}$.

As a result of this competition, only a small fraction of $^{\bullet}CCl_3$ and $:CCl_2$ generated during the photolysis was trapped effectively. The relative trapping efficiency was optimized by using a high concentration of 2,3-dimethyl-2-butene (e.g., 0.1 M).

Kinetic Analysis of TCCl2 Formation. From the mechanism of Table 1, the observed TCCl2 production rate (Figures 5 and 6) can be expressed as (reaction R23)

$$\frac{d[TCCl2]}{dt} = k_{R23}[:CCl_2][T] \tag{10}$$

Since the initial rates of TCCl2 formation were measured after the induction period, reaction steps involving dissolved oxygen (reactions R5 and R18) can be ignored. The reverse reaction of reaction R12 is not considered because the chloride production is small during the initial period. Three different cases of electron transfers to CCl_4 are treated separately: (i) sequential one-electron (free e_{cb}^-) transfers (reactions R7 and R9); (ii) a simultaneous two-electron (free e_{cb}^-) transfer (reaction R11); (iii) sequential one-electron (trapped electron, $>Ti^{III}$) transfers (reactions R8 and R10). The derived kinetic rate equations for each case under the two extreme conditions of low and high light intensities are summarized in Table 2. We present the derivation of the kinetic expression for TCCl2 production for only case iii, since it represents the most complex mechanism.

The concentration of $:CCl_2$ during the photolysis can be assumed to be in steady-state according to eq 11:

$$k_{R12}[CCl_3^-] = k_{R23}[:CCl_2][T] + k_{R25}[:CCl_2][H_2O] + 2k_{R22}[:CCl_2]^2 \tag{11}$$

The term reflecting the bimolecular recombination of $:CCl_2$ is negligible relative to the other terms such that

$$[:CCl_2] = \frac{k_{R12}[CCl_3^-]}{k_{R23}[T] + k_{R25}[H_2O]} = k_a[CCl_3^-] \tag{12}$$

where

$$k_a = \frac{k_{R12}}{k_{R23}[T] + k_{R25}[H_2O]}$$

Similar steady-state analysis for $[CCl_3^-]$ yields

$$\frac{d[CCl_3^-]}{dt} = k_{R10}[^{\bullet}CCl_3][>Ti^{III}] - k_{-R10}[CCl_3^-] - k_{R12}[CCl_3^-] - k_{R21}[CCl_3^-][H^+] \approx 0$$

$$[CCl_3^-] = \frac{k_{R10}[^{\bullet}CCl_3][>Ti^{III}]}{k_{-R10} + k_{R12} + k_{R21}[H^+]} = f_3([H^+])[^{\bullet}CCl_3][>Ti^{III}] \tag{13}$$

where

$$f_3([H^+]) = \frac{k_{R10}}{k_{-R10} + k_{R12} + k_{R21}[H^+]}$$

The corresponding steady-state treatment for $^{\bullet}CCl_3$ yields

$$\frac{d[^{\bullet}CCl_3]}{dt} = k_{R8}[CCl_{4,ad}][>Ti^{III}] - k_{R10}[^{\bullet}CCl_3][>Ti^{III}] + k_{-R10}[CCl_3^-] - 2k_{R16}[^{\bullet}CCl_3]^2 - [^{\bullet}CCl_3]\sum k_i[S_i] \approx 0 \tag{14}$$

where k_i and S_i refer to the reactions that deplete $^{\bullet}CCl_3$, such as reactions R17−19. Since the $[^{\bullet}CCl_3]^2$ term is negligible, we can rewrite eq 14 as

$$[^{\bullet}CCl_3] = \frac{k_{R8}[CCl_{4,ad}][>Ti^{III}] + k_{-R10}[CCl_3^-]}{k_{R10}[>Ti^{III}] + \sum k_i[S_i]} \tag{15}$$

When the back-reaction rate of reaction R10 is slow compared to the rate of reaction R8, eq 15 can be simplified to

$$[^{\bullet}CCl_3] = \frac{k_{R8}[CCl_{4,ad}][>Ti^{III}]}{k_{R10}[>Ti^{III}] + \sum k_i[S_i]} \quad (16)$$

The trapped electron, $>Ti^{III}$, concentration is given by

$$\frac{d[>Ti^{III}]}{dt} = k_{R6}[Ti^{IV}][e_{cb}^-] - k_{-R6}[>Ti^{III}] - k_{R8}[CCl_{4,ad}][>Ti^{III}] - k_{R10}[^{\bullet}CCl_3][>Ti^{III}] + k_{-R10}[CCl_3^-] \approx 0 \quad (17)$$

$$[>Ti^{III}] = \frac{k_{R6}[Ti^{IV}][e_{cb}^-] + k_{-R10}[CCl_3^-]}{k_{-R6} + k_{R8}[CCl_{4,ad}] + k_{R10}[^{\bullet}CCl_3]} \quad (18)$$

The second term in the numerator of eq 18 can be neglected, because the electron trapping reaction (reaction R6) is very fast compared to the reverse reaction of reaction R10.[27] The third term in the denominator of eq 18 is much smaller than the second term, since the steady-state concentration of trichloromethyl radical should be much lower than the adsorbed CCl_4 concentration. Therefore, eq 18 is reduced to

$$[>Ti^{III}] = \frac{k_{R6}[Ti^{IV}][e_{cb}^-]}{k_{-R6} + k_{R8}[CCl_{4,ad}]} \quad (19)$$

The steady-state concentration of free charge-carriers under illumination can be related to the absorbed light intensity, I_{abs} as follows:[26]

$$\frac{d[h_{vb}^+]}{dt} = I_{abs} - k_{R13}[h_{vb}^+][H_2O] - k_{R15}[h_{vb}^+][e_{cb}^-] \approx 0 \quad (20)$$

$$I_{abs} = k_{R13}[e_{cb}^-][H_2O] + k_{R15}[e_{cb}^-]^2 \quad \text{(by assuming } [h_{vb}^+] \approx [e_{cb}^-]) \quad (21)$$

for low light intensities

$$[e_{cb}^-] = \frac{I_{abs}}{k_{R13}[H_2O]} = \frac{I_{abs}}{k'_{R13}} \quad (\text{where } k'_{R13} = k_{R13}[H_2O]) \quad (22)$$

and for high light intensities

$$[e_{cb}^-] = \left(\frac{I_{abs}}{k_{R15}}\right)^{1/2} \quad (23)$$

Combining eqs 10, 12, 13, 16, 19, 22, and 23 yields for low light intensities

$$\frac{d[TCCl2]}{dt} = k_{3L}I_{abs}^{\ 2}\frac{\frac{k_{R8}}{k_{-R6}}[CCl_{4,ad}]}{\left(1 + \frac{k_{R8}}{k_{-R6}}[CCl_{4,ad}]\right)^2} \quad (24)$$

where

$$k_{3L} = \frac{k_a k_{R23} k_{R6}^{\ 2} f_3([H^+])}{k'_{R13}^{\ 2} k_{-R6} \sum k_i[S_i]}[Ti^{IV}]^2[T]$$

and for high light intensities

$$\frac{d[TCCl2]}{dt} = k_{3H}I_{abs}^{\ 1/2}\frac{\frac{k_{R8}}{k_{-R6}}[CCl_{4,ad}]}{\left(1 + \frac{k_{R8}}{k_{-R6}}[CCl_{4,ad}]\right)} \quad (25)$$

where

$$k_{3H} = \frac{k_a k_{R23} k_{R6} f_3([H^+])}{k_{R10} k_{R15}^{\ 1/2}}[Ti^{IV}][T]$$

Discussion

From our experimental results, we conclude that both $^{\bullet}CCl_3$ and $:CCl_2$ are formed via one- and two-electron reductions of CCl_4 on illuminated TiO_2 surfaces. Similar observations of distinct one- and two-electron pathways were made by Bahnemann et al.[7a] during the photoreduction of halothane (2-bromo-2-chloro-1,1,1-trifluoroethane). However, they noted that the presence of surficial Pt deposits on the TiO_2 was essential for the two-electron reduction pathway to occur.

The effect of water on the production rate of TCCl2 and TCCl3 (Figure 3) can be interpreted in terms of the role of the hydroxyl radical in the hole-scavenging mechanism. Efficient hole scavenging is essential for maximizing conduction-band electron transfer, since most of the photogenerated electrons in the colloidal TiO_2 system recombine with holes. Two hole-scavenging mechanisms are currently being discussed among researchers: direct and indirect hole transfers[28,29]

$$h_{vb}^+ + D \rightarrow D^{\bullet +} \quad \text{direct hole transfer} \quad (26)$$

$$h_{vb}^+ + H_2O \text{ (or } >Ti^{IV}OH^-) \rightarrow {}^{\bullet}OH \text{ (or } >Ti^{IV}OH^{\bullet}) \xrightarrow{DH} D^{\bullet} + H_2O \quad \text{indirect hole transfer} \quad (27)$$

where D and DH represent electron donors. The trap (2,3-dimethyl-2-butene) can serve as an electron donor for both direct and indirect hole transfer. However, the data in Figure 3 indicate that indirect hole transfer, which involves water molecules and surficial hydroxyl radicals, is a more efficient hole-scavenging pathway. Adding 2-methyl-2-propanol or 2-propanol as additional hole scavengers had little effect on the production rate of TCCl2 and TCCl3. Similar conclusions, which were based on H−D kinetic isotope effects, were drawn previously.[18,28] When $[H_2O] \geq 1$ M, the hole-scavenging efficiency leveled off.

Since Cl^- production was negligible over the range 0.0 M < $[H_2O]$ < 1.0 M, in which the production of TCCl2 and TCCl3 was rapid (Figure 3), most $:CCl_2$ and $^{\bullet}CCl_3$ radicals were trapped with no further degradation. However, when $[H_2O] = 10$ M, the $[Cl^-]$ yield was 200 μM which corresponded to ~50 μM CCl_4 degraded. This implies that CCl_4 degradation is significant only with the presence of an excess amount of water. The principal role of water in CCl_4 degradation does not seem to be as a source of hydroxyl radicals, since the hole-scavenging efficiency leveled off at $[H_2O] \geq 1$ M. This indicates that the hydrolysis of the intermediate $:CCl_2$ may play a primary role in the complete degradation of CCl_4.

Dichlorocarbene is known to undergo hydrolysis (reaction 8) while trichloromethyl radical does not. The hydrolysis reaction of dichlorocarbene has been studied in detail by Robinson,[30] who proposed the following mechanism:

$$:CCl_2 \xrightarrow{2OH^-,\, H_2O} CO + 2H^+ + 2Cl^- \quad (28)$$

$$CO \xrightarrow{OH^-(slow)} HCOO^- \quad (29)$$

As $[H_2O]$ increases, reaction 28 competes effectively with trapping reaction 4. As a result, the [TCCl2] decreased as $[H_2O]$ increased from 1 to 10 M while [TCCl3] continued to increase (Figure 3). The rapid increase in the CCl_4 degradation rate at high pH, as shown in Figures 7 and 8, can be attributed primarily to the base-catalyzed reaction of eq 28.

In our previous study,[18] we attributed the enhanced rate of CCl_4 reduction at high pH solely to the larger thermodynamic driving force of conduction band (CB) electron transfer to CCl_4, which is a result of normal Nernstian behavior. However, this study indicates a more complex process. Increasing TCCl2 production coincides with decreasing TCCl3 production at log $[OH^-]_{add} < -4.0$ (Figure 7). In this region, total chloride production from reductive dechlorination and hydrolysis remains constant. The fate of $^{\bullet}CCl_3$ should be independent of pH. This implies that a larger thermodynamic driving force for CB electron transfer increasingly favors a two-electron transfer over a one-electron transfer to CCl_4. For the range of log $[OH^-]_{add} > -3.5$, however, both the production of TCCl2 and TCCl3 rapidly decrease with a concurrent increase in total Cl^- production.

The two-electron transfer represented by the reaction of eq 2 can be broken into several steps as follows.

$$CCl_4 + e_{cb}^- \rightarrow {}^{\bullet}CCl_3 + Cl^- \quad (30)$$

$$^{\bullet}CCl_3 + e_{cb}^- \leftrightarrow CCl_3^- \quad (31)$$

$$CCl_3^- \leftrightarrow :CCl_2 + Cl^- \quad (32)$$

Equation 32 has been shown to be the rate-determining step in the basic hydrolysis of chloroform.[31] If the photogenerated dichlorocarbene is rapidly scavenged by reaction 28 at high pH, the equilibrium of reaction 32 shifts to the right side of the equation. Sequentially, so does that of reaction 31. As a result, we can expect more trichloromethyl radicals to lead to dichlorocarbene with increasing pH. However, we cannot expect TCCl2 production to increase continuously with pH, as is shown in Figure 7, because the hydrolysis reaction (reaction 28) starts to compete with reaction 4. From the above argument, we can say that increasing pH has a dual effect on CCl_4 degradation. One part of this effect is the shift in the CB electron potential to a more negative value according to Nernstian behavior, which results in an increase in the electron-transfer rate, and the other part is an increase in the rate of hydrolysis of dichlorocarbene. This latter effect leads to the full degradation of CCl_4 and favors dichlorocarbene formation over trichloromethyl radical formation by shifting the equilibria of reactions 31 and 32.

The relative effect of pH on intermediate formation (Figure 9) is consistent with the data shown in Figure 7. The intermediates are formed at pH 2.7, where both TCCl2 and TCCl3 are detected, but they are absent at pH 12.4, where neither TCCl2 nor TCCl3 are seen. Hexachloroethane (C_2Cl_6) and perchloroethylene (C_2Cl_4) are formed through the recombination of two trichloromethyl radicals (reaction 6) and two dichlorocarbenes (reaction 9), respectively. Chloroform ($CHCl_3$) could be formed through two pathways.

$$^{\bullet}CCl_3 + (CH_3)_2CHOH \rightarrow CHCl_3 + (CH_3)_2\dot{C}OH \quad (33)$$

$$CCl_3^- + H^+ \rightarrow CHCl_3 \quad (34)$$

Since all of the chlorinated intermediates were derived from either $:CCl_2$ or $^{\bullet}CCl_3$, their formation should be directly correlated with the formation of TCCl2 and TCCl3. At pH 12.4, trapped conduction-band electron transfer to CCl_4 seems to lead to the formation of dichlorocarbene, which is then rapidly hydrolyzed with little chance of recombination.

Oxygen also plays a dual role. It competes as an electron acceptor with CCl_4, and it serves as a reactant (reaction 5), which is essential for the release of three Cl^- ions from trichloromethyl radical. The proposed mechanism for this pathway based on pulse radiolysis of CCl_4 is as follows:[11]

$$CCl_4 + e_{aq}^- \rightarrow {}^{\bullet}CCl_3 + Cl^- \quad (35)$$

$$O_2 + e_{aq}^- \rightarrow O_2^{\bullet -} \quad (36)$$

$$O_2^{\bullet -} + H^+ \leftrightarrow HO_2^{\bullet} \quad (37)$$

$$^{\bullet}CCl_3 + O_2 \rightarrow {}^{\bullet}OOCCl_3 \quad (38)$$

$$2{}^{\bullet}OOCCl_3 \rightarrow O_2 + 2{}^{\bullet}OCCl_3 \quad (39)$$

$$HO_2^{\bullet} + {}^{\bullet}OCCl_3 \rightarrow O_2 + HOCCl_3 \quad (40)$$

$$^{\bullet}OCCl_3 + (CH_3)_3COH \rightarrow HOCCl_3 + {}^{\bullet}CH_2(CH_3)_2COH \quad (41)$$

$$HOCCl_3 \rightarrow COCl_2 + H^+ + Cl^- \quad (42)$$

$$COCl_2 + H_2O \rightarrow CO_2 + 2H^+ + 2Cl^- \quad (43)$$

Since the production of TCCl3 in the presence of air is retarded relative to that of TCCl2 (Figure 4), we conclude that either $^{\bullet}CCl_3$ or the intermediate carbon-centered radical in reaction 3 is scavenged by oxygen addition to some extent while $:CCl_2$ is not. Therefore, some of the CCl_4 could be degraded completely by following reactions 35−43. However, reactions 35−43 do not seem to be the dominant pathway for CCl_4 degradation in the UV/TiO_2 system for the following reasons: (i) carbon tetrachloride is fully degraded in the absence of dissolved oxygen; (ii) the total chloride production is significant only in the presence of excess water and at high pH; (iii) the relative distribution of the intermediates and their pH dependence cannot be explained by a mechanism involving only the trichloromethyl radical. The two-electron transfer to CCl_4 and the subsequent hydrolysis of dichlorocarbene seem to be a main path for CCl_4 degradation in the UV/TiO_2 system.

The resulting kinetic expressions for cases i and iii (from Table 2) predict the observed light intensity dependence of TCCl2 production: the production rate is proportional to I_{abs}^2 at low light intensities and $I_{abs}^{1/2}$ at high light intensities. However, cases ii, which involves the simultaneous two-electron transfer, does not explain the square-root dependence of TCCl2 production at high light intensities. On the basis of this analysis, CCl_4 appears to be reduced through sequential one-electron transfers instead of a simultaneous two-electron transfer.

The initial TCCl2 production rates (Figure 5a) show apparent Langmuir−Hinshelwood-type kinetics with respect to the initial CCl_4 concentration. Even though both cases i and iii predict the observed light intensity dependence, they have different $[CCl_4]$ dependencies. Case i shows that the reaction rate will be proportional to $[CCl_{4,ad}]$ under both low and high light intensities. On the other hand, case iii predicts that the concentration dependence should be different between the low and high light intensity conditions especially at higher CCl_4 concentrations. The production rates under the low-intensity irradiation should start to decrease at higher CCl_4 concentration according to case iii. This behavior can be rationalized in terms of the competition for limited trapped electrons between $^{\bullet}CCl_3$

and CCl_4. However, the low-intensity limit of case iii is not consistent with the experimental observations (Figure 5a) because we failed to see any significant difference in the concentration dependence between the low and high light intensity cases. However, we cannot rule out the possibility that case iii is operative at high light intensities. We note that the high-intensity limit of case iii takes the typical form of Langmuir−Hishelwood kinetics.

On the basis of the above argument, we conclude that the reduction of CCl_4 proceeds through consecutive *free* electron transfers at low light intensities (case i) and through the consecutive *trapped* or *free* electron transfers at high light intensities (cases i and iii). Even though Rothenberger et al.[27] showed that the electron trapping was a very rapid process (τ < 30 ps) in colloidal (diameter 12 nm) particles of TiO_2 in aqueous solution where there were no added electron donors and acceptors, the *free* electron transfer at the interface could be possible in the present colloidal system, which drastically differs from that of Rothenberger et al. The photoinduced charge-transfer at the semiconductor/liquid interface is strongly influenced by various parameters such as the colloid surface condition, the presence of electron donors and acceptors, and the size and the crystallinity of the semiconductor particle.[27,32] With an excess amount of electron donors (traps) and acceptors (CCl_4 and O_2) available on the surface, the interfacial *free* electron transfer may compete with the fast electron trapping at the surface site.

Conclusions

Photoinduced electron transfer to CCl_4 on colloidal TiO_2 surfaces is shown to involve both one-electron and two-electron reduction pathways producing $^{\bullet}CCl_3$ and $:CCl_2$, respectively, as intermediates. Even though both pathways lead to the degradation of CCl_4, the two-electron reduction appears to be the principal pathway, leading to complete degradation. Since the two-electron pathway involves the formation of dichlorocarbene, which readily undergoes base-catalyzed hydrolysis, pH is found to be a critical experimental variable that controls the rate of degradation of CCl_4. At high pH, the degradation rate is greatly enhanced and no intermediates (e.g., C_2Cl_4 and C_2Cl_6) are detected. The presence of water is essential for the degradation of CCl_4 because it provides an efficient hole-scavenging pathway and because it is critical for the hydrolysis of dichlorocarbene. Comparing the results of a kinetic model derived from a proposed mechanism to the observed light-intensity dependence indicates that the two-electron transfer pathway is a consecutive electron−electron transfer and not a single two-electron transfer. The mechanism of CCl_4 degradation proposed in this work may provide useful information for further studies of the photoreduction of perhalogenated organic compounds in TiO_2/UV systems.

Acknowledgment. Financial support from the Advanced Research Projects Agency (ARPA) and the Office of Naval Research (ONR) (Grant N0014-92-J-1901) under the auspices of the Department of Defense−University Research Initiative Program (DOD-URI) is gratefully acknowledged.

References and Notes

(1) (a) Fujishima, A.; Honda, K. *Nature* **1972**, *238*, 37. (b) Grätzel, M. *Acc. Chem. Res.* **1981**, *14*, 376.
(2) Fox, M. A. *Acc. Chem. Res.* **1983**, *16*, 314.
(3) (a) Borgarello, E.; Serpone, N.; Emo, G.; Harris, R.; Pelizzetti, E.; Minero, C. *Inorg. Chem.* **1986**, *25*, 4499. (b) Foster, N. S.; Noble, R. D.; Koval, C. A. *Environ. Sci. Technol.* **1993**, *27*, 350.
(4) (a) Ollis, D. F., Al-Ekabi, H., Eds. *Photocatalytic Purification and Treatment of Water and Air;* Elsevier: Amsterdam, 1993. (b) Hoffmann, M. R.; Martin, S. T.; Choi, W.; Bahnemann, D. W. *Chem. Rev.* **1995**, *95*, 69.
(5) Frank, S. N.; Bard, A. J. *J. Phys. Chem.* **1977**, *81*, 1484.
(6) (a) Choi, W.; Termin, A.; Hoffmann, M. R. *Angew. Chem., Int. Ed. Engl.* **1994**, *33*, 1091. (b) Choi, W.; Termin, A.; Hoffmann, M. R. *J. Phys. Chem.* **1994**, *98*, 13669.
(7) (a) Bahnemann, D. W.; Mönig, J.; Chapman, R. *J. Phys. Chem.* **1987**, *91*, 3782. (b) Hilgendorff, M.; Hilgendorff, M.; Bahnemann, D. W. In *Environmental Aspects of Electrochemistry and Photoelectrochemistry*; Tomkiewicz, M., Haynes, R., Yoneyama, H., Hori, Y., Eds.; The Electrochemical Society: Pennington, NJ, 1993; pp 112−121.
(8) Chemseddine, A.; Boehm, H. P. *J. Mol. Catal.* **1990**, *60*, 295.
(9) Filby, W. G.; Mintas, M.; Güsten, H. *Ber. Bunsen-Ges. Phys. Chem.* **1981**, *85*, 189.
(10) Moser, J.; Grätzel, M. *J. Am. Chem. Soc.* **1983**, *105*, 6547.
(11) (a) Asmus, K.-D.; Bahnemann, D.; Krischer, K.; Lal, M.; Mönig, J. *Life Chem. Rep.* **1985**, *3*, 1. (b) Mönig, J.; Bahnemann, D.; Asmus, K.-D. *Chem.-Biol. Interact.* **1983**, *45*, 15. (c) Köster, R.; Asmus, K.-D. *Z. Naturforsch* **1971**, *26b*, 1104.
(12) (a) Bhatnagar, A.; Cheung, H. M. *Environ. Sci. Technol.* **1994**, *28*, 1481. (b) Hua, I.; Hoffmann, M. R. *Environ. Sci. Technol.*, in press.
(13) Criddle, C. S.; McCarty, P. L. *Environ. Sci. Technol.* **1991**, *25*, 973.
(14) (a) Lambert, F. L.; Hasslinger, B. L.; Franz, R. N., III. *J. Electrochem. Soc.: Electrochem. Sci. Technol.* **1975**, *122*, 737. (b) Wawzonek, S.; Duty, R. C. *J. Electrochem. Soc.* **1961**, *108*, 1135. (c) Kolthoff, I. M.; Lee, T. S.; Stocesova, D.; Parry, E. P. *Anal. Chem.* **1950**, *22*, 521.
(15) Zhou, X.-L.; Cowin, J. P. Submitted to *J. Phys. Chem.*
(16) (a) Kriegman-King, M. R.; Reinhard, M. *Environ. Sci. Technol.* **1992**, *26*, 2198. (b) Kriegman-King, M. R.; Reinhard, M. *Environ. Sci. Technol.* **1994**, *28*, 692. (c) Hooker, P. D.; Klabunde, K. J. *Environ. Sci. Technol.* **1994**, *28*, 1243.
(17) Matheson, L. J.; Tratnyek, P. G. *Environ. Sci. Technol.* **1994**, *28*, 2045.
(18) Choi, W.; Hoffmann, M. R. *Environ. Sci. Technol.* **1995**, *29*, 1646.
(19) Heller, H. G.; Langan, J. R. *J. Chem. Soc. Perkin Trans.* **1981**, *2*, 341.
(20) Doering, W. v. E.; Henderson, W. A., Jr. *J. Am. Chem. Soc.* **1958**, *80*, 5274.
(21) Biemann, K. *Mass Spectrometry−Organic Chemical Applications*; McGraw Hill: New York, 1962.
(22) Martin, S. T.; Herrmann, H.; Choi, W.; Hoffmann, M. R. *J. Chem. Soc., Faraday Trans.* **1994**, *90*, 3315.
(23) (a) Egerton, T. A.; King, C. J. *J. Oil Colour Chem. Assoc.* **1979**, *62*, 386. (b) Okamoto, K.-I.; Yamamoto, Y.; Tanaka, H.; Itaya, A. *Bull. Chem. Soc. Jpn.* **1985**, *58*, 2023.
(24) Westcott, C. C. *pH Measurements*; Academic Press: Orlando, FL, 1978.
(25) Kormann, C.; Bahnemann, D. W.; Hoffmann, M. R. *Environ. Sci. Technol.* **1991**, *25*, 494.
(26) Turchi, C. S.; Ollis, D. F. *J. Catal.* **1990**, *122*, 178.
(27) Rothenberger, G.; Moser, J.; Grätzel, M.; Serpone, N.; Sharma, D. K. *J. Am. Chem. Soc.* **1985**, *107*, 8054.
(28) Cunningham, J.; Srijaranai, S. *J. Photochem. Photobiol., A: Chem.* **1988**, *43*, 329.
(29) Stafford, U.; Gray, K. A.; Kamat, P. V. *J. Phys. Chem.* **1994**, *98*, 6343.
(30) Robinson, E. A. *J. Chem. Soc.* **1961**, 1663.
(31) Kirmse, W. *Carbene Chemistry; Organic Chemistry−A Series of Monographs, Vol. 1;* Academic Press: New York, 1964.
(32) Frei, H.; Fitzmaurice, D. J.; Grätzel, M. *Langmuir* **1990**, 6, 198.

JP951431K